Minimal energy cost to initialize a bit with tolerable error

Yu-Han Ma,[1] Jin-Fu Chen,[1,2,3] C. P. Sun,[1,2,*] and Hui Dong[1,†]

[1]*Graduate School of China Academy of Engineering Physics, No. 10 Xibeiwang East Road, Haidian District, Beijing, 100193, China*

[2]*Beijing Computational Science Research Center, Beijing 100193, China*

[3]*School of Physics, Peking University, Beijing, 100871, China*

(Received 9 January 2022; accepted 25 August 2022; published 7 September 2022)

Landauer's principle imposes a fundamental limit on the energy cost to perfectly initialize a classical bit, which is only reached under the ideal operation with infinitely long time. The question on the cost in the practical operation for a bit has been raised under the constraint by the finiteness of operation time. We discover a raise-up of energy cost by $\mathcal{L}^2(\epsilon)/\tau$ from the Landaeur's limit ($k_BT\ln 2$) for a finite-time τ initialization of a bit with an error probability ϵ. The thermodynamic length $\mathcal{L}(\epsilon)$ between the states before and after initializing in the parametric space increases monotonously as the error decreases. For example, in the constant dissipation coefficient (γ_0) case, the minimal additional cost is $0.997k_BT/(\gamma_0\tau)$ for $\epsilon = 1\%$ and $1.288k_BT/(\gamma_0\tau)$ for $\epsilon = 0.1\%$. Furthermore, the optimal protocol to reach the bound of minimal energy cost is proposed for the bit initialization realized via a finite-time isothermal process.

DOI: 10.1103/PhysRevE.106.034112

I. INTRODUCTION

Initializing memory is a necessary process in computation [1–6] for further information processing and inevitably requires an expense of energy. Landauer derived a fundamental limit of energy cost for such a process that a minimal $k_BT\ln 2$ (k_B is the Boltzmann constant) heat will be dissipated to the environment of temperature T for erasing one bit information [1,7–11]. Such a limit is only reached with two idealities, infinitely long operation time and perfect initialization, which are unfortunately impossible for practical devices.

However, in real-world circumstances, initializing bits in finite time is critical for speeding up computation processes. A finite-time Landauer's principle was, in turn, proposed to reveal that the corresponding energy cost is significantly increased with the decrease of the erasure time [11–17] and the first ideality is overcome. Besides the classical computation, information erasure is also essential for quantum computation whose basic unit is the quantum bit (qubit) [5,18–20]. When the qubit is initialized to a desired state, there are unavoidable errors in practice. Errors also occur in the implementation of gate operations. To ensure the overall low error, the lower error of initialization allows more quantum gate operations. A critical error probability is typically required in the quantum computation process, e.g., 1% for error correction [21–23]. Therefore, the second ideality is not necessary.

It is, therefore, natural to ask what is the minimal energy cost to initialize a bit with tolerable errors within finite time? In a recent study, Zhen *et al.* [24] answered this question by presenting a lower bound on the energy cost of a bit reset. It should be noted that, in addition to the lower bound of the energy cost itself, how to achieve the minimal energy cost is another important question that needs to be explored in practical initialization of bits. In this paper, we tackle this problem by exploiting the geometry framework of quantum thermodynamics [25–31] to study the finite-time information erasure in a bit. The erasure here is realized by driving the bit in a thermal bath.

This work is organized as follows. In Sec. II, we utilize the master equation to study the work cost for erasing the information of a bit. When driving is not applied infinitely slowly, the additional work required in the erasure process is obtained. In Sec. III, we first quantify the additional work with the thermodynamic length $\mathcal{L}$ (depending on the error probability ϵ), which serves as an important geometric quantity to characterize nonequilibrium dissipation [25–31]. Then we discover an analytical trade-off relation among the energy cost, erasure time, and error probability with the asymptotic behavior of $\mathcal{L}$. Furthermore, for applications, we demonstrate the error-probability-dependent optimal erasure protocol to achieve the minimal energy cost for bit initialization. The numerical validations of the trade-off are also presented. In Sec. IV, we discuss the temperature dependence of the total work cost for initializing the bit. The conclusion and a discussion are given in Sec. V.

II. WORK COST FOR INITIALIZING A BIT

A classical bit or a qubit can be physically modeled as a two-level system, and the information encoded by the logical state "0" ("1") is represented by the ground state $|g\rangle$ (excited state $|e\rangle$) of the two-level system. Before the erasure process, we assume that the bit contains one bit of information and stays at the maximum mixed state $\rho_i = (|e\rangle\langle e| + |g\rangle\langle g|)/2$. In the ideal erasure, the bit is restored into the logical state "0" perfectly, namely $\rho_f = |g\rangle\langle g|$. However, in a practical process,

*suncp@gscaep.ac.cn

†hdong@gscaep.ac.cn

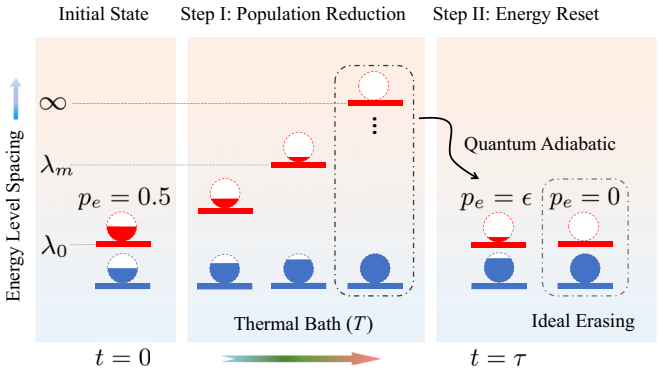

FIG. 1. Schematic of finite-time information erasure for a bit. The ground state and excited state of the bit represent the logical states "0" and "1," respectively. The energy level spacing of the bit λ is first tuned from $\lambda_0 = 0$ to $\lambda_f = \lambda_m$ when it is in contact with a thermal bath of temperature T. Then the energy level spacing of the bit is tuned back to 0 quantum adiabatically. In the ideal erasure process with $\lambda_m \to \infty$, the bit is completely erased to the logical state "'0" with the population in the logical state "1" $p_e = 0$.

the bit is generally erased to $\rho_f = \epsilon|e\rangle\langle e| + (1-\epsilon)|g\rangle\langle g|$ with an error probability ϵ.

To implement the initialization, the energy-level spacing of the two-level system is tuned by a control parameter $\lambda(t)$ under the Hamiltonian $H(t) = \lambda(t)\sigma_z/2$ with the Pauli matrix $\sigma_z = |e\rangle\langle e| - |g\rangle\langle g|$. The Planck's constant is taken as $\hbar = 1$ hereafter for brevity. As illustrated in Fig. 1, the entire information erasure process is designed with two steps as follows.

(i) **Population reduction** by increasing the energy-level spacing λ from $\lambda_0 = 0$ to λ_m. The bit is coupled to a thermal bath of inverse temperature $\beta = 1/(k_B T)$.

(ii) **Energy reset** by quantum adiabatically decreasing the energy-level spacing of the bit back to λ_0 with no thermal bath. The first step is designed to reduce the population in the excited state and the second step aims to restore the system's Hamiltonian for future operations.

Since quantum coherent operations are not involved in the above erasure process, there is no fundamental difference between the initialization of qubits and classical bits in our case. It is worth noting that, at the beginning and the end of the above erasure process, the energy-level spacing of the bit is set to $\lambda_0 = 0$. The two logical states of the bit are degenerate in energy. To distinguish the bit states for further computational operations, an additional degree of freedom is needed, such as an electrical charge in the case of charge bits. The following discussion does not rely on this degree of freedom since it does not affect the energy cost of interest during the bit initialization process.

The total work performed in the erasure process with duration τ is $W(\tau) = \int_0^\tau \dot{W} dt$ with the erasure power $\dot{W} \equiv \mathrm{tr}(\rho \dot{H})$ [32,33], which is explicitly written as

$$\dot{W} = \frac{\dot{\lambda}(t)}{2}[2p_e(t) - 1]. \tag{1}$$

The probability for the bit on the excited state $p_e(t)$ is governed by the master equation [34] $\dot{p}_e = \mathscr{L}(p_e)$. For the bit in contact with a bosonic heat bath, $\mathscr{L}(p_e)$ reads [34]

$$\mathscr{L}(p_e) = \gamma\{n(\lambda) - [2n(\lambda) + 1]p_e\}, \tag{2}$$

where $n(\lambda) = 1/(e^{\beta\lambda} - 1)$ is the average particle number of the bath mode with energy λ and the dissipation coefficient $\gamma = \gamma(\lambda)$ is determined by the bath spectral density [34].

A. Work done in the quasistatic erasure process

The work done in the quasistatic erasure process is equal to the free energy change ΔF between the states of the bit before and after initializing. In the quasistatic population reduction process, the bit always satisfies the thermal equilibrium distribution $p_e^{\mathrm{eq}}(\lambda) = e^{-\beta\lambda}/(1 + e^{-\beta\lambda})$.

When the energy-level spacing of the bit is tuned from $\lambda_0 \to \lambda_m$, the corresponding quasistatic work $W_{\mathrm{qs}}^{(1)} \equiv \int_{\lambda_0}^{\lambda_m}[p_e^{\mathrm{eq}}(\lambda) - 1/2]d\lambda$ is obtained as

$$W_{\mathrm{qs}}^{(1)} = \beta^{-1} \ln\left(\frac{1 + e^{-\beta\lambda_0}}{1 + e^{-\beta\lambda_m}}\right) - \frac{1}{2}(\lambda_m - \lambda_0). \tag{3}$$

Then the energy level spacing of the bit is tuned back to λ_0 adiabatically in the energy reset process, and the work done $W_{\mathrm{qs}}^{(2)} \equiv \int_{\lambda_m}^{\lambda_0}[p_e^{\mathrm{eq}}(\lambda_m) - 1/2]d\lambda$ is

$$W_{\mathrm{qs}}^{(2)} = \frac{e^{-\beta\lambda_m}}{1 + e^{-\beta\lambda_m}}(\lambda_0 - \lambda_m) + \frac{1}{2}(\lambda_m - \lambda_0). \tag{4}$$

Therefore, the total quasistatic work done in these two processes $W_{\mathrm{qs}} \equiv W_{\mathrm{qs}}^{(1)} + W_{\mathrm{qs}}^{(2)}$ is

$$W_{\mathrm{qs}} = \Delta F = \beta^{-1}[\ln 2 - S(\epsilon)]. \tag{5}$$

Here, we chose $\lambda_0 = 0$ and defined $\epsilon \equiv e^{-\beta\lambda_m}/(1 + e^{-\beta\lambda_m})$ as the error probability. $S(\epsilon) = -\epsilon \ln \epsilon - (1-\epsilon)\ln(1-\epsilon)$ is the Shannon entropy of the final state and $\beta^{-1}\ln 2$ is the work cost in the ideal erasure process ($\epsilon = 0$) as stated by *Landauer's principle* [1]. Since the entropy $S(\epsilon)$ is an increasing function for $0 \leqslant \epsilon \leqslant 1/2$, more work is required to achieve lower error probability (smaller ϵ).

B. Irreversible work and irreversible power

To evaluate the finite-time effect, we define the irreversible work

$$W_{\mathrm{ir}}(\tau) \equiv W(\tau) - \Delta F = \int_0^\tau \dot{W}_{\mathrm{ir}}(t)dt. \tag{6}$$

Here, the irreversible power [30,31] is

$$\dot{W}_{\mathrm{ir}} = \dot{\lambda}(t)\big\{p_e(t) - p_e^{\mathrm{eq}}[\lambda(t)]\big\}, \tag{7}$$

and $p_e^{\mathrm{eq}}[\lambda(t)] = e^{-\beta\lambda(t)}/[1 + e^{-\beta\lambda(t)}]$ is the excited-state population in the instantaneous thermal equilibrium distribution. Finding the minimal energy cost for erasing the information stored in a bit is now converted to deriving the lower bound of the irreversible work.

With the instantaneous equilibrium distribution, Eq. (2) is rewritten as

$$\left[1 + \frac{1 - 2p_e^{\mathrm{eq}}(\lambda)}{\gamma\tau}\frac{d}{d\widetilde{t}}\right]p_e = p_e^{\mathrm{eq}}(\lambda), \tag{8}$$

with the dimensionless time $\widetilde{t} \equiv t/\tau$. The series expansion solution of this equation with respect to $\gamma\tau$ follows as:

$$p_e = \left[1 + \frac{1-2p_e^{\rm eq}(\lambda)}{\gamma\tau}\frac{d}{d\widetilde{t}}\right]^{-1} p_e^{\rm eq}(\lambda) \tag{9}$$

$$= \sum_{n=0}\left[-\frac{1-2p_e^{\rm eq}(\lambda)}{\gamma\tau}\frac{d}{d\widetilde{t}}\right]^{n} p_e^{\rm eq}(\lambda). \tag{10}$$

In the slow-driving regime with $\gamma(\lambda)\tau \gg 1$, we obtain the excited population $p_e(t)$ to the first order of $1/(\gamma\tau)$ as

$$p_e \approx p_e^{\rm eq}(\lambda) - \frac{1-2p_e^{\rm eq}(\lambda)}{\gamma}\frac{\partial p_e^{\rm eq}}{\partial\lambda}\dot{\lambda}. \tag{11}$$

The irreversible power $\dot{W}_{\rm ir} = \dot{\lambda}(t)(p_e - p_e^{\rm eq})$ is thus explicitly obtained as

$$\dot{W}_{\rm ir} = \beta\gamma^{-1}\frac{(1-e^{-\beta\lambda})e^{-\beta\lambda}}{(1+e^{-\beta\lambda})^3}\dot{\lambda}^2. \tag{12}$$

The typical form of the dissipation coefficient $\gamma = \gamma_0\lambda^\alpha$ will be used in the following discussion, where γ_0 is a constant, and $\alpha \in [0,1)$, $\alpha = 1$, and $\alpha > 1$ correspond to the sub-Ohmic, Ohmic, and super-Ohmic spectrums of the bath, respectively [35,36].

III. MINIMAL WORK COST AND OPTIMAL ERASURE PROTOCOL

The irreversible work $W_{\rm ir}$ is bounded from below by $W_{\rm ir} \geqslant \mathcal{L}^2/\tau$ with the thermodynamic length $\mathcal{L} \equiv \int_0^\tau \sqrt{\dot{W}_{\rm ir}}dt$ [25–31,37,38], which is the geometric distance in the parametric space and independent of the specific erasure protocol of $\lambda(t)$.

According to Eq. (12), with the typical dissipation coefficient $\gamma(\lambda) = \gamma_0\lambda^\alpha$, the thermodynamic length of the population reduction process is explicitly obtained in terms of ϵ as

$$\mathcal{L}(\epsilon) = \sqrt{\beta^{(\alpha-1)}\gamma_0^{-1}}f_\alpha(\epsilon) \tag{13}$$

with the dimensionless function

$$f_\alpha(\epsilon) \equiv \int_0^{\ln(\epsilon^{-1}-1)}\sqrt{\frac{(1-e^{-x})e^{-x}}{x^\alpha(1+e^{-x})^3}}dx. \tag{14}$$

The upper limit of the integral in Eq. (14) reflects the dependence of $\mathcal{L}(\epsilon)$ on the error probability ϵ.

The precise lower bound for irreversible work is denoted as

$$W_{\rm ir}^{\rm min}(\epsilon) \equiv \frac{\mathcal{L}^2(\epsilon)}{\tau}. \tag{15}$$

Particularly, in the constant dissipation coefficient case ($\alpha = 1$), $W_{\rm ir}^{\rm min} = 0.997k_BT/(\gamma_0\tau)$ for $\epsilon = 1\%$ and $W_{\rm ir}^{\rm min} = 1.288k_BT/(\gamma_0\tau)$ for $\epsilon = 0.1\%$.

A. Trade-off among work cost, erasure time, and error probability

Utilizing the asymptotic behavior of the thermodynamic length (see Appendix A for a detailed proof)

$$\mathcal{L}(\epsilon) \approx \mathcal{L}(0) - 2\sqrt{\beta^{(\alpha-1)}\gamma_0^{-1}\epsilon\ln^{-\alpha}(\epsilon^{-1})}, \tag{16}$$

with $\mathcal{L}(0)$ the thermodynamic length for the perfect erasing ($\epsilon = 0$), the bound on the irreversible work $W_{\rm ir} \geqslant \mathcal{L}^2(\epsilon)/\tau$ becomes

$$\frac{W_{\rm ir}\tau}{\mathcal{L}^2(0)} + \mu_\alpha\sqrt{\epsilon\ln^{-\alpha}(\epsilon^{-1})} \geqslant 1. \tag{17}$$

Here, the $\mathcal{O}(\epsilon)$ term was ignored and $\mu_\alpha \equiv 4/f_\alpha(0)$ is a dimensionless constant determined solely by the bath spectrum.

The above Eq. (17) quantitatively reveals a trade-off relation among irreversible work $W_{\rm ir}$, erasure time τ, and error probability ϵ. For the special case of the perfect erasing ($\epsilon = 0$), such a trade-off recovers the result $W_{\rm ir} \geqslant \mathcal{L}^2(0)/\tau$ obtained in the recent studies on the finite-time Landauer's principle [7,11,13–16,39,40]. A similar result was obtained in a recent study [24]. Differently, in this work, we take use of the thermodynamic length to characterize the minimal work cost for bit initialization and will focus on how to geometrically determine the optimal protocol to achieve this lower bound.

In addition, we emphasize here that Eq. (17) serves as the overall lower bound for irreversible work in the slow-driving regime since the approximation of the thermodynamic length in Eq. (16) is always smaller than the exact thermodynamic length for arbitrary ϵ (see Appendix A for details).

We plot the analytical lower bound

$$\widetilde{W}_{\rm ir}^{\rm min} \equiv \frac{\mathcal{L}^2(0)[1-\mu_\alpha\sqrt{\epsilon\ln^{-\alpha}(\epsilon^{-1})}]}{\tau} \tag{18}$$

of Eq. (17) as the surface in Fig. 2(a) for the Ohmic spectrum case with $\alpha = 1$. In the simulation, we always use the following parameters: $\gamma_0 = 1$ and $\beta = 1$. The monotonicity of the surface indicates that more extra energy cost is required to accomplish the erasure with higher accuracy and shorter operation time. The trade-offs associated with the sub-Ohmic and super-Ohmic spectrum cases are illustrated in Appendix B.

B. Optimal erasure protocol

The optimal erasure protocol $\lambda(t)$ applied to initializing the bit for minimal work cost satisfies $\sqrt{\dot{W}_{\rm ir}} = \mathcal{L}(\epsilon)/\tau$ [25–31,37,38], which is explicitly written as, by utilizing Eq. (12),

$$\frac{d\lambda}{d\widetilde{t}} = \mathcal{L}(\epsilon)\left[\frac{\beta(1-e^{-\beta\lambda})e^{-\beta\lambda}}{\gamma_0\lambda^\alpha(1+e^{-\beta\lambda})^3}\right]^{-\frac{1}{2}}, \tag{19}$$

where $\tilde{t} \equiv t/\tau$ is the dimensionless time.

The exact optimal protocol is numerically obtained by solving the above differential equation with the boundary conditions $\lambda(\tilde{t}=0) = 0$ and $\lambda(\tilde{t}=1) = \lambda_m$. In Fig. 2(b), we illustrate the optimal protocols for cases with $\alpha = 1$ for $\epsilon = 10^{-1}$ (black solid curve), $\epsilon = 10^{-2}$ (blue dashed curve), and $\epsilon = 10^{-4}$ (red dash-dotted curve), respectively. The optimal protocols in the cases with $\alpha = 0, 2$ are demonstrated in Appendix B.

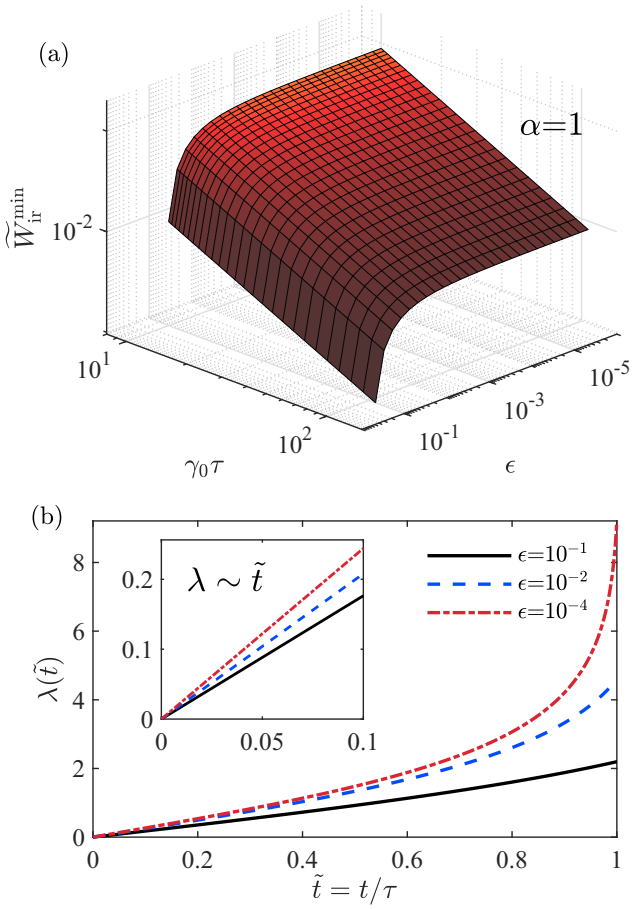

FIG. 2. (a) Analytical trade-off among irreversible work, erasure time τ and error probability ϵ in the Ohmic spectrum case ($\alpha = 1$). The surface is plotted with the analytical lower bound ($\widetilde{W}_{\rm ir}^{\rm min}$) of Eq. (17) with $f_1(0) = 0.9433$ [Eq. (A1)]. (b) Optimal protocol of $\lambda(\tilde{t})$ in the Ohmic spectrum case ($\alpha = 1$) with different error probabilities ϵ. The black solid curve, blue dashed curve, and red dash-dotted curve represent the optimal protocol for $\epsilon = 10^{-1}$, $\epsilon = 10^{-2}$, and $\epsilon = 10^{-4}$, respectively. The scaling of the optimal protocol in the initial stage $\lambda(\tilde{t} \ll 1) \sim \tilde{t}$ is illustrated in the inset figure. The parameters $\beta = 1$ and $\gamma_0 = 1$ are used to plot this figure.

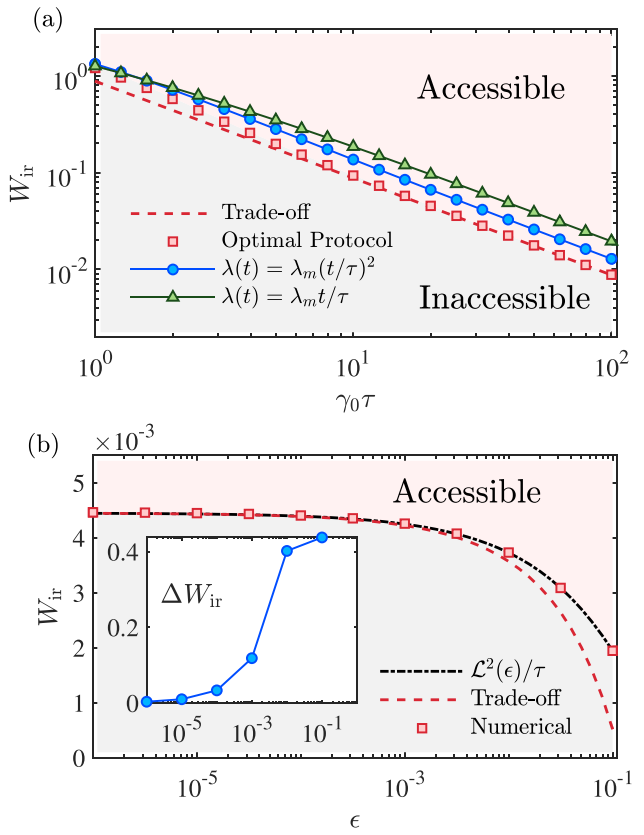

FIG. 3. (a) Irreversible work as a function of the erasure time τ in the Ohmic spectrum case ($\alpha = 1$), where $\epsilon = 10^{-4}$ is fixed. The red squares represent the exact minimal irreversible work associated with the optimal erasure protocol. The blue dot curve (green triangle curve) is obtained numerically with the erasure protocol chosen as $\lambda(t) = \lambda_m(t/\tau)^2$ ($\lambda(t) = \lambda_m t/\tau$), where $\lambda_m = \beta^{-1}\ln(\epsilon^{-1} - 1)$. The red dashed curve is plotted with the analytical lower bound $\widetilde{W}_{\rm ir}^{\rm min}$. (b) Minimal irreversible work as a function of error probability ϵ in the case with $\alpha = 1$, where $\tau = 200$ is fixed. The red squares are obtained numerically with the optimal erasure protocol, while the black dash-dotted curve and red dashed curve represent the precise lower bound $W_{\rm ir}^{\rm min} = \mathcal{L}^2(\epsilon)/\tau$ and the analytical lower bound $\widetilde{W}_{\rm ir}^{\rm min}$, respectively. The additional work $\Delta W_{\rm ir}(\epsilon)$ required to reduce the error probability ϵ by an order of magnitude is plotted in the inset figure. In this figure, we use $\beta = 1$ and $\gamma_0 = 1$.

In the initial stage ($\tilde{t} = t/\tau \ll 1$) of the population reduction process, noticing $\lambda(\tilde{t}) \ll 1$, Eq. (19) is approximated as

$$\frac{d\lambda}{d\tilde{t}} \approx \mathcal{L}(\epsilon)\beta^{-1}\sqrt{8\gamma_0}\lambda^{\frac{\alpha-1}{2}}. \tag{20}$$

By straightforward calculation, one obtains the optimal protocol

$$\lambda(\tilde{t} \ll 1) = [2(3-\alpha)^2\gamma_0\beta^{-2}\mathcal{L}^2(\epsilon)]^{\frac{1}{3-\alpha}}\tilde{t}^{\frac{2}{3-\alpha}}, \tag{21}$$

where the power exponent of $\tilde{t}$ is only determined by the bath spectrum parameter α. This implies that, in the initial stage ($\tilde{t} \ll 1$) of the erasure process, the optimal protocols scale as $\lambda \sim \tilde{t}^{2/(3-\alpha)}$. The inset figure shows the optimal protocol $\lambda \sim \tilde{t}$ in the present case ($\alpha = 1$). We stress that the solution of Eq. (19) with respect to $\tilde{t}$ is independent of the erasure time. Therefore, for given erasure processes (fixed α, ϵ) with different duration τ, the required optimal protocol $\lambda(t)$ can be directly obtained by performing variable substitution $\tilde{t} \to t/\tau$ on the fixed optimal protocol (with respect to $\tilde{t}$).

C. Numerical validations of the trade-off

We solve the exact minimal irreversible work numerically from Eqs. (2) and (7) to validate the analytical trade-off in Eq. (17). The irreversible work is illustrated in Fig. 3(a) as a function of the erasure time with $\epsilon = 10^{-4}$. The red squares represent the numerical results corresponding to the optimal erasure protocol and the analytical lower bound $\widetilde{W}_{\rm ir}^{\rm min}$ is plotted with red dash-dotted curve. The analytical trade-off, exhibiting the typical $1/\tau$-scaling of irreversibility [7,11,26,41–48], is in good agreement with the numerical results in the long-time regime of $\gamma_0\tau \gg 1$. In the short-time

regime (beyond the slow-driving regime), the higher-order terms of $1/(\gamma_0\tau)$ in the expansion of $\dot{W}_{\rm ir}$ cannot be ignored anymore, and thus the minimal irreversible work deviates from the $1/\tau$ scaling [45,46,49].

To demonstrate the dependence of irreversible work on the erasure protocol, the exact numerical irreversible work related to two erasure protocols, $\lambda(t) = \lambda_m(t/\tau)^2$ and $\lambda(t) = \lambda_m t/\tau$ [$\lambda_m = \beta^{-1}\ln(\epsilon^{-1} - 1)$], are illustrated with the blue dotted curve and green triangle curve, respectively. The irreversible work corresponding to these two protocols are larger in comparison with the minimal irreversible work achieved with the optimal protocol (red squares). Since the irreversible work cannot be less than that associated with the optimal protocol with any erasure protocol, we denote the light gray area below the red squares as the inaccessible regime of the irreversible work. In this sense, the light red area above the red squares is accessible.

The exact minimal irreversible work as a function of the error probability is marked with the red squares in Fig. 3(b) for fixed duration $\tau = 200$. The irreversible work increases for lower the error probability. Similar to Fig. 3(a), the two areas separated by the red squares (achieved with the optimal protocol) represent the accessible and inaccessible regions. The black dash-dotted curve represents the precise bound of the irreversible work $W_{\rm ir}^{\rm min}$ characterized by the exact thermodynamic length, which agrees well with the exact numerical results in the entire plotted range of ϵ. The fact that the red dashed curve ($\widetilde{W}_{\rm ir}^{\rm min}$) approaches to the black dash-dotted curve ($W_{\rm ir}^{\rm min}$) in the low error probability regime ($\epsilon \ll 1$) is consistent with the approximation condition used to obtain Eq. (17).

In addition, we introduce the following normalized quantity

$$\Delta W_{\rm ir}(\epsilon) \equiv \frac{W_{\rm ir}^{\rm min}(\epsilon) - W_{\rm ir}^{\rm min}(10\epsilon)}{W_{\rm ir}^{\rm min}(0)} \tag{22}$$

to evaluate the additional work required to reduce the error probability ϵ by an order of magnitude. As demonstrated in the inset figure of Fig. 3(b) $\Delta W_{\rm ir}$ decreases rapidly with the error probability. We remark that it typically requires less additional work to reduce the error probability in the low-ϵ regime, noticing the plateau at the $\epsilon \leqslant 10^{-4}$ region.

The numerical results confirm that the analytical trade-off (red dashed curve) approaches the precise lower bound (black dash-dotted curve) with the error probability $\epsilon \ll 1$. Beyond the regime $\epsilon \ll 1$ or $\gamma\tau \gg 1$, one can observe from Figs. 2(a) and 2(b) that all the exact minimal irreversible work (red squares) locates above the red dashed curve. This implies that our analytical trade-off (17) may have a wider applicable scope beyond the slow-driving regime.

IV. OPTIMAL BATH TEMPERATURE FOR MINIMAL WORK COST

Unlike the quasistatic work done [Eq. (5)] for the initializing bit that is linearly dependent on the bath temperature, the temperature dependence of the irreversible work is determined by the specific bath spectrum as implied by Eq. (13). This inspires us to discuss the temperature dependence of the minimal work cost in the erasure process in this section.

Combining Eqs. (5), (6), (13), and (15), the minimal work cost $W^{\rm min}(\tau) \equiv \Delta F + W_{\rm ir}^{\rm min}$ in the erasure process, in terms of the thermodynamic length, follows as

$$W^{\rm min}(\tau) = \beta^{-1}S_{\rm era} + \frac{\mathcal{L}^2(\epsilon)}{\tau} \tag{23}$$

$$= \beta^{-1}S_{\rm era} + \frac{\beta^{(\alpha-1)}\gamma_0^{-1}f_\alpha^2(\epsilon)}{\tau}, \tag{24}$$

where $S_{\rm era} \equiv \ln 2 - S(\epsilon)$. For given erasure time τ, in the sub-Ohmic and Ohmic spectrum cases with $\alpha \leqslant 1$, the work done is a monotonically increasing function of the temperature T. Thus, the minimal work cost tends to zero at zero temperature.

However, for arbitrary $\alpha > 1$, $W^{\rm min}$ has a lower bound, which is achieved with $\partial W^{\rm min}/\partial\beta = 0$, namely,

$$-\beta^{-2}S_{\rm era} + (\alpha - 1)\frac{\beta^{(\alpha-2)}\gamma_0^{-1}f_\alpha^2(\epsilon)}{\tau} = 0. \tag{25}$$

The optimal temperature is solved from this equation as

$$\beta_\alpha^{-1} = \left[\frac{(\alpha-1)f_\alpha^2(\epsilon)}{\gamma_0\tau S_{\rm era}}\right]^{\frac{1}{\alpha}} \equiv \widetilde{T}_\alpha, \tag{26}$$

where the Boltzmann constant is taken as $k_B = 1$ for brevity. Therefore, when the bath temperature is set as the above optimal one, the minimal work cost is

$$W_\alpha^{\rm min} \equiv W^{\rm min}|_{T=\widetilde{T}_\alpha} = \frac{\alpha\widetilde{T}S_{\rm era}}{\alpha - 1}, \tag{27}$$

which decreases with $\tau^{1/\alpha}$. This indicates that we can choose suitable bath temperature to reduce the work cost for erasing information in the bit. Particularly, in the case with $\alpha = 2$, the minimal work cost, i.e., $W_2^{\rm min} = 2f_2(\epsilon)\sqrt{S_{\rm era}/\gamma_0\tau}$, decreases with $\sqrt{\tau}$.

V. CONCLUSION AND DISCUSSIONS

In summary, we studied the finite-time information erasure in a bit with tolerable errors. A trade-off among irreversible work, erasure time, and error probability is obtained for nonequilibrium erasure processes. This trade-off relation, characterized by the thermodynamic length, reveals that reducing the erasure time and error probability requires an additional energy cost. For practical purposes, we found the optimal erasure protocol associated with the minimal work cost to initialize a bit. The exact numerical calculations validate the trade-off and show that it is quite tight in the long-time regime with low error probability. In addition, we also discussed the optimal bath temperature, determined by the bath spectrum, for the minimal work cost. The presented results hold for both classical bits and qubits without coherence.

These findings indicate that the spectrum of the bath, by affecting the dissipation dynamics, has important influences on the initialization of the bits. To achieve the minimal energy consumption, it is necessary to choose the optimal erasure protocol and set the optimal temperature of the bath according to different bath spectrum. This study shall bring

additional insights to the practical optimization of information processing in computation. As possible extensions, the influences of different bath spectrum, quantum coherence of the qubit [17,39,50], and fast-driving of the erasure process [11,31,51,52] on the trade-off and the optimal erasure protocol obtained in the current work can be taken into future consideration.

ACKNOWLEDGMENTS

This work is supported by the National Natural Science Foundation of China (NSFC) (Grants No. 11534002, No. 11875049, No. U1730449, No. U1530401, and No. U1930403), the National Basic Research Program of China (Grants No. 2016YFA0301201), and the China Postdoctoral Science Foundation (Grant No. BX2021030).

APPENDIX A: ASYMPTOTIC EXPRESSION OF THE THERMODYNAMIC LENGTH

In this section, we discuss the asymptotic expression of the thermodynamic length $\mathcal{L}(\epsilon)$ with respect to ϵ. For the perfect erasure $\epsilon = 0$, we have $\mathcal{L}(0) = \sqrt{\beta^{(\alpha-1)}\gamma_0^{-1}} f_\alpha(0)$ with

$$f_\alpha(0) = \int_0^\infty \sqrt{\frac{(1-e^{-x})e^{-x}}{x^\alpha(1+e^{-x})^3}}dx = \begin{cases} 1.1981 & \alpha = 0, \\ 0.9433 & \alpha = 1, \\ 1.0914 & \alpha = 2. \end{cases} \tag{A1}$$

For general erasure processes, $f_\alpha(\epsilon)$ can be reexpressed in terms of $f_\alpha(0)$ as $f_\alpha(\epsilon) = f_\alpha(0) - I_\alpha(\epsilon)$ with

$$I_\alpha(\epsilon) \equiv \int_{\ln(\epsilon^{-1}-1)}^\infty \sqrt{\frac{(1-e^{-x})e^{-x}}{x^\alpha(1+e^{-x})^3}}dx. \tag{A2}$$

We further use a new integral variable $y \equiv e^{-x}$ to rewrite Eq. (A2) as

$$I_\alpha(\epsilon) = \int_0^\epsilon (-\ln y)^{-\alpha/2}\sqrt{\frac{(1-y)}{y(1+y)^3}}dy, \tag{A3}$$

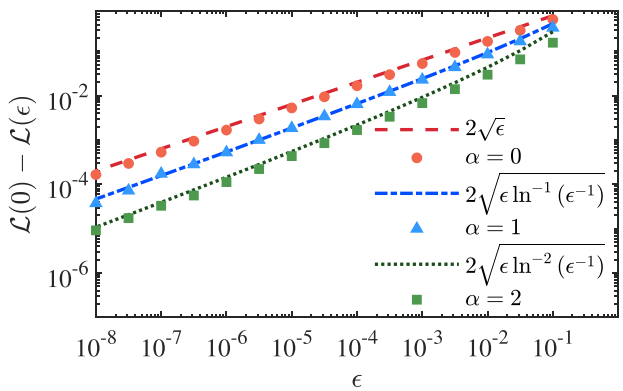

FIG. 4. $\mathcal{L}(0) - \mathcal{L}(\epsilon)$ as functions of ϵ with $\alpha = 0, 1, 2$. In this plot, we choose $\beta = 1$, $\gamma_0 = 1$.

which is expanded into series form with respect to y as

$$I_\alpha(\epsilon) = \int_0^\epsilon (-\ln y)^{-\alpha/2}\left[\frac{1}{\sqrt{y}} - 2\sqrt{y} + \mathcal{O}\left(y^{\frac{3}{2}}\right)\right]dy. \tag{A4}$$

Noticing

$$\sqrt{\frac{(1-y)}{y(1+y)^3}} \leqslant \sqrt{\frac{1}{y}}, \tag{A5}$$

we find $I_\alpha(\epsilon)$ is bounded from below by the first term of its series expansion as

$$I_\alpha(\epsilon) \leqslant \int_0^\epsilon (-\ln y)^{-\alpha/2}\frac{1}{\sqrt{y}}dy \tag{A6}$$

$$= 2\sqrt{\epsilon}[\ln(\epsilon^{-1})]^{-\frac{\alpha}{2}} - \alpha\int_0^\epsilon \frac{[\ln(y^{-1})]^{-\frac{\alpha}{2}-1}}{\sqrt{y}}dy \tag{A7}$$

$$\leqslant 2\sqrt{\epsilon}[\ln(\epsilon^{-1})]^{-\frac{\alpha}{2}}. \tag{A8}$$

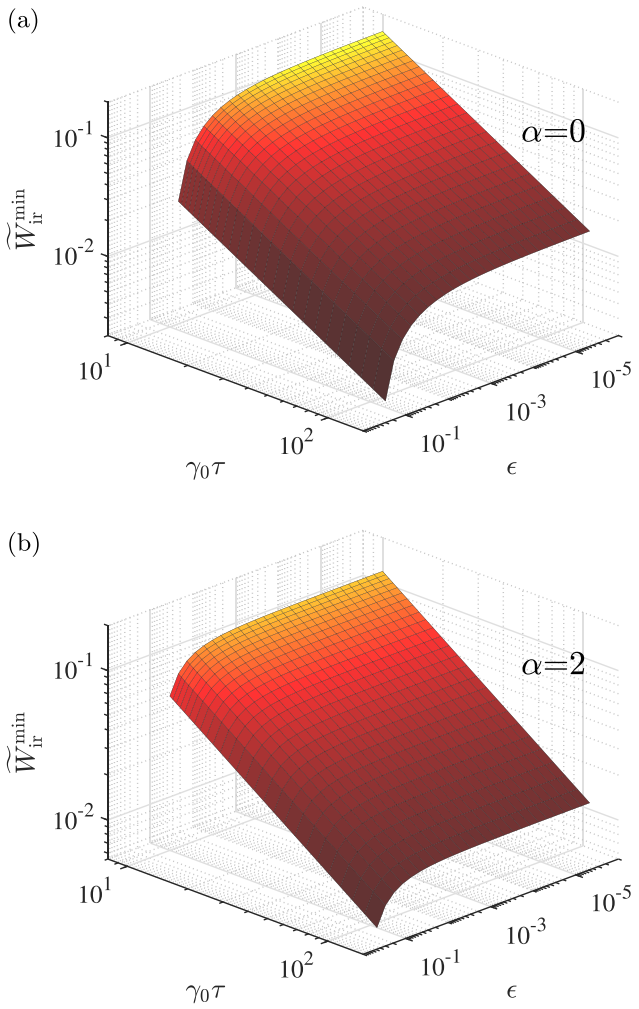

FIG. 5. Analytical trade-off among irreversible work, erasure time τ and error probability ϵ in (a) sub-Ohmic spectrum case ($\alpha = 0$) and (b) super-Ohmic spectrum case ($\alpha = 2$). The surface is plotted with the analytical lower bound ($\widetilde{W}_{\rm ir}^{\rm min}$) of Eq. (17) and the parameters $\beta = 1$ and $\gamma_0 = 1$ are used to plot this figure.

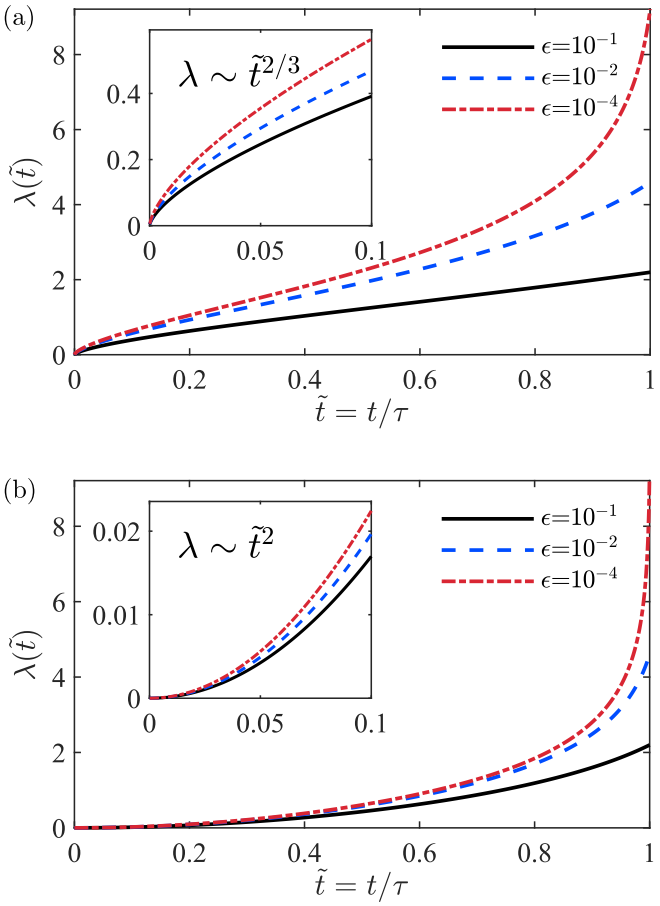

FIG. 6. Optimal protocol of $\lambda(\tilde{t})$ in the cases with (a) $\alpha = 0$ and (b) $\alpha = 2$ for different error probability ϵ. The black solid curve, blue dashed curve, and red dash-dotted curve represent the optimal protocols for $\epsilon = 10^{-1}$, $\epsilon = 10^{-2}$, and $\epsilon = 10^{-4}$, respectively. The scaling of the optimal protocol in the initial stage $\lambda(\tilde{t} \ll 1) \sim \tilde{t}^{2/(3-\alpha)}$ is illustrated in the inset figure. In this plot, $\gamma_0 = 1$ and $\beta = 1$ are used.

Therefore, the thermodynamic length $\mathcal{L}(\epsilon) = \sqrt{\beta^{(\alpha-1)}\gamma_0^{-1}} f_\alpha(\epsilon)$ has a lower bound as

$$\mathcal{L}(\epsilon) = \sqrt{\beta^{(\alpha-1)}\gamma_0^{-1}}[f_\alpha(0) - I_\alpha(\epsilon)] \tag{A9}$$

$$\geqslant \sqrt{\beta^{(\alpha-1)}\gamma_0^{-1}}\left[f_\alpha(0) - 2\sqrt{\epsilon}(-\ln\epsilon)^{-\alpha/2}\right] \tag{A10}$$

$$= \mathcal{L}(0) - 2\sqrt{\beta^{(\alpha-1)}\gamma_0^{-1}\epsilon \ln^{-\alpha}(\epsilon^{-1})}. \tag{A11}$$

We stress that this inequality for $\mathcal{L}(\epsilon)$ is quite tight in the low error probability regime ($\epsilon \ll 1$). As shown in Fig. 4, the asymptotic expression

$$\mathcal{L}(\epsilon) \approx \mathcal{L}(0) - 2\sqrt{\beta^{(\alpha-1)}\gamma_0^{-1}\epsilon \ln^{-\alpha}(\epsilon^{-1})}, \tag{A12}$$

of the thermodynamic length (lines) agrees well with the exact numerical results (dots) obtained from Eq. (13).

APPENDIX B: TRADE-OFFS AND OPTIMAL ERASURE PROTOCOLS FOR $\alpha = 0, 2$

The trade-offs associated with the sub-Ohmic ($\alpha = 0$) and super-Ohmic ($\alpha = 2$) spectrum case are illustrated in Fig. 5. By numerically solving Eq. (19), the exact optimal protocols for $\alpha = 0, 2$ are plotted in Fig. 6. The scaling $\lambda \sim \tilde{t}^{2/(3-\alpha)}$ in the initial stage ($\tilde{t} = t/\tau \ll 1$) is illustrated in the inset figures.

[1] R. Landauer, IBM J. Res. Dev. **5**, 183 (1961).
[2] C. H. Bennett, IBM J. Res. Dev. **17**, 525 (1973).
[3] W. H. Zurek, Nature (London) **341**, 119 (1989).
[4] C. H. Bennett, D. P. DiVincenzo, and J. A. Smolin, Phys. Rev. Lett. **78**, 3217 (1997).
[5] M. Nielsen, *Quantum Computation and Quantum Information* (Cambridge University Press, Cambridge, England, 2000).
[6] J. M. R. Parrondo, J. M. Horowitz, and T. Sagawa, Nat. Phys. **11**, 131 (2015).
[7] A. Bérut, A. Arakelyan, A. Petrosyan, S. Ciliberto, R. Dillenschneider, and E. Lutz, Nature (London) **483**, 187 (2012).
[8] Y. Jun, M. Gavrilov, and J. Bechhoefer, Phys. Rev. Lett. **113**, 190601 (2014).
[9] J. P. S. Peterson, R. S. Sarthour, A. M. Souza, I. S. Oliveira, J. Goold, K. Modi, D. O. Soares-Pinto, and L. C. Céleri, Proc. R. Soc. A. **472**, 20150813 (2016).
[10] L. L. Yan, T. P. Xiong, K. Rehan, F. Zhou, D. F. Liang, L. Chen, J. Q. Zhang, W. L. Yang, Z. H. Ma, and M. Feng, Phys. Rev. Lett. **120**, 210601 (2018).
[11] S. Dago, J. Pereda, N. Barros, S. Ciliberto, and L. Bellon, Phys. Rev. Lett. **126**, 170601 (2021).
[12] G. Diana, G. B. Bagci, and M. Esposito, Phys. Rev. E **87**, 012111 (2013).
[13] P. R. Zulkowski and M. R. DeWeese, Phys. Rev. E **89**, 052140 (2014).
[14] P. R. Zulkowski and M. R. DeWeese, Phys. Rev. E **92**, 032113 (2015).
[15] K. Proesmans, J. Ehrich, and J. Bechhoefer, Phys. Rev. Lett. **125**, 100602 (2020).
[16] K. Proesmans, J. Ehrich, and J. Bechhoefer, Phys. Rev. E **102**, 032105 (2020).
[17] T. Van Vu and K. Saito, Phys. Rev. Lett. **128**, 010602 (2022).
[18] R. P. Feynman, Opt. News **11**, 11 (1985).
[19] D. P. DiVincenzo, Science **270**, 255 (1995).
[20] D. P. DiVincenzo, Fortschr. Phys.: Prog. Phys. **48**, 771 (2000).
[21] A. M. Steane, Phys. Rev. Lett. **77**, 793 (1996).
[22] D. S. Wang, A. G. Fowler, and L. C. L. Hollenberg, Phys. Rev. A **83**, 020302(R) (2011).

[23] S. Zhang, Y. Lu, K. Zhang, W. Chen, Y. Li, J.-N. Zhang, and K. Kim, Nat. Commun. **11**, 587 (2020).
[24] Y.-Z. Zhen, D. Egloff, K. Modi, and O. Dahlsten, Phys. Rev. Lett. **127**, 190602 (2021).
[25] G. Ruppeiner, Phys. Rev. A **20**, 1608 (1979).
[26] P. Salamon and R. S. Berry, Phys. Rev. Lett. **51**, 1127 (1983).
[27] R. Gilmore, Phys. Rev. A **30**, 1994 (1984).
[28] L. Diósi, K. Kulacsy, B. Lukács, and A. Rácz, J. Chem. Phys. **105**, 11220 (1996).
[29] G. E. Crooks, Phys. Rev. Lett. **99**, 100602 (2007).
[30] D. A. Sivak and G. E. Crooks, Phys. Rev. Lett. **108**, 190602 (2012).
[31] J.-F. Chen, C. P. Sun, and H. Dong, Phys. Rev. E **104**, 034117 (2021).
[32] R. Alicki, J. Phys. A: Math. Gen. **12**, L103 (1979).
[33] H. T. Quan, Y. X. Liu, C. P. Sun, and F. Nori, Phys. Rev. E **76**, 031105 (2007).
[34] H.-P. Breuer and F. Petruccione, *The Theory of Open Quantum Systems,* (Oxford University Press, New York, 2007), Chap. 3, Sec. 3.4.
[35] A. J. Leggett, S. Chakravarty, A. T. Dorsey, M. P. Fisher, A. Garg, and W. Zwerger, Rev. Mod. Phys. **59**, 1 (1987).
[36] M. Scandi and M. Perarnau-Llobet, Quantum **3**, 197 (2019).
[37] K. Brandner and K. Saito, Phys. Rev. Lett. **124**, 040602 (2020).
[38] P. Abiuso, H. J. D. Miller, M. Perarnau-Llobet, and M. Scandi, Entropy **22**, 1076 (2020).
[39] H. J. D. Miller, G. Guarnieri, M. T. Mitchison, and J. Goold, Phys. Rev. Lett. **125**, 160602 (2020).
[40] T. Van Vu and Y. Hasegawa, Phys. Rev. Lett. **126**, 010601 (2021).
[41] P. Salamon, A. Nitzan, B. Andresen, and R. S. Berry, Phys. Rev. A **21**, 2115 (1980).
[42] K. Sekimoto and S.-I. Sasa, J. Phys. Soc. Jpn. **66**, 3326 (1997).
[43] T. Schmiedl and U. Seifert, Europhys. Lett. **81**, 20003 (2008).
[44] M. Esposito, R. Kawai, K. Lindenberg, and C. V. Van den Broeck, Phys. Rev. Lett. **105**, 150603 (2010).
[45] Y.-H. Ma, D. Xu, H. Dong, and C.-P. Sun, Phys. Rev. E **98**, 042112 (2018).
[46] Y.-H. Ma, R.-X. Zhai, J. Chen, C. P. Sun, and H. Dong, Phys. Rev. Lett. **125**, 210601 (2020).
[47] Y.-H. Ma, Entropy **22**, 1002 (2020).
[48] H. Yuan, Y.-H. Ma, and C. P. Sun, Phys. Rev. E **105**, L022101 (2022).
[49] Y.-H. Ma, D. Xu, H. Dong, and C.-P. Sun, Phys. Rev. E **98**, 022133 (2018).
[50] S. Su, J. Chen, Y. Ma, J. Chen, and C. Sun, Chin. Phys. B **27**, 060502 (2018).
[51] V. Cavina, P. A. Erdman, P. Abiuso, L. Tolomeo, and V. Giovannetti, Phys. Rev. A **104**, 032226 (2021).
[52] Y.-H. Ma, H. Dong, and C. P. Sun, Commun. Theor. Phys. **73**, 125101 (2021).